

Deintercalation of dimethylsulphoxide intercalated kaolinites – a DTA/TGA and Raman spectroscopic study

R.L. Frost^{a,*}, J. Kristof^b, E. Horvath^c, J.T. Kloprogge^a

^a Centre for Instrumental and Developmental Chemistry, Queensland University of Technology, 2 George Street, GPO Box 2434, Brisbane, Queensland 4001, Australia

^b Department of Analytical Chemistry, University of Veszprem, PO Box 158, H8201 Veszprem, Hungary

^c Research Group for Analytical Chemistry, Hungarian Academy of Sciences, PO Box 158, H8201 Veszprem, Hungary

Received 28 July 1998; received in revised form 30 October 1998; accepted 18 November 1998

Abstract

The deintercalation of dimethylsulphoxide intercalated kaolinites was studied using a combination of thermal analysis techniques and Raman spectroscopy. Thermal analysis shows three endotherms at 77°, 117° and 173°C attributed to the loss of water and the loss of DMSO in two stages. The use of a thermal stage enabled Raman spectra of the deintercalation process to be obtained in situ at elevated temperatures. The Raman spectra of the DMSO intercalated kaolinites show two bands at 3620 and 3660 cm⁻¹ for the DMSO intercalated low defect kaolinite and 3620 and 3664 cm⁻¹ for the high defect intercalated kaolinite. The 3620 cm⁻¹ band is attributed to the inner hydroxyl of the kaolinite and shows no change upon deintercalation. The 3660 and 3664 cm⁻¹ bands are attributed to the inner surface hydroxyls of the kaolinite hydrogen bonded to the DMSO. The intensity of these bands decreases upon thermal treatment and at the same time, the bands at 3695 and 3684 cm⁻¹ increase in intensity. These changes clearly show that the 3660 cm⁻¹ band is attributable to the inner surface hydroxyls hydrogen bonded to the DMSO. Deintercalation may also be followed by the decrease in intensity of the CH-stretching bands. The application of the DTA/TGA patterns to determine the appropriate temperatures for Raman spectroscopy of the dimethylsulphoxide proved most useful. © 1999 Elsevier Science B.V. All rights reserved.

Keywords: Dimethylsulphoxide (DMSO); DRIFT; High defect kaolinite; Intercalation; Kaolinite; Low defect kaolinite; Raman microscopy; Thermal analysis

1. Introduction

Clay minerals can interact with both organic and inorganic chemicals through a number of mechanisms such as adsorption, intercalation and cation exchange. The basic principles of intercalation reactions have been elucidated for kaolinite (Al(OH)₄·2SiO₂) by

Lagaly [1]. The reactive guest molecules enter the interlayer spaces and expand the kaolinite layers, essentially making the kaolinite into a single layered mineral. The inserting molecule breaks the hydrogen bonds formed between the kaolinite hydroxyl groups and the oxygens of the next adjacent siloxane layer. The inserting molecule then forms hydrogen bonds with either the hydrophobic surface of the kaolinite (the siloxane layer) or the hydrophilic part of the kaolinite surface (the hydroxyl surfaces of the gibb-

*Corresponding author. Tel.: +61-7-3864-2407; fax: +61-7-3864-1804; e-mail: r.frost@qut.edu.au

site-like layer). A further possibility exists in that the inserting or adsorbing molecule may interact with the end surfaces of the kaolinites. The reactive molecules have been classified into groups according to the point of clay interaction. Group A consists of those compounds that can form strong hydrogen bonds to the siloxane layers, e.g. hydrazine, urea, formamide, and acetamide. Group B consists of molecules with strong dipole interactions that can interact with the silicate layers and includes molecules such as dimethylsulphoxide [(CH₃)₂SO] abbreviated to DMSO. Group C consists of the alkali salts of short chain fatty acids, in particular acetic and propionic acids [2].

The reason why DMSO is so successful at distinguishing the clay minerals is that the kaolins expand from 7.2 to 11.2 Å. This expansion of the kaolin minerals including halloysite, kaolinite, dickite and nacrite, by DMSO followed by deintercalation results in an increase in the disorder of the kaolin [3,4]. Intercalation of DMSO into kaolinite provides a method for the incorporation of other alkali and alkaline metal salts into the kaolin by replacement of the DMSO [5,6]. When the kaolinite is expanded with DMSO, a three-dimensional ordering incorporating the DMSO into the interlamellar space occurs [7–9]. It has been proposed that when this three-dimensional ordering occurs, the DMSO molecule is locked into the kaolinite surfaces firstly by hydrogen bonding of the S=O to the gibbsite-like hydroxyls and by a coordination of the sulphur to the oxygens of the siloxane surface. Such three-dimensional ordering then alters the molecular motion of the methyl groups of the DMSO [9–11]. Stable, three-dimensionally ordered complexes were formed from a highly ordered kaolinite ($d(001) = 7.20 \text{ \AA}$) with dimethylsulphoxide [12–14]. Removal of the intercalated organic compounds by drying or by water washing produced an 8.40 Å hydrate with its ordered layer stacking essentially unchanged.

The application of Raman microscopy to the study of intercalated kaolinites has proven most useful [15–19]. For example, for the potassium acetate intercalate an additional Raman band, attributed to the inner surface hydroxyl groups strongly hydrogen bound to the acetate, was observed at 3605 cm^{-1} with the concomitant loss of intensity in the bands at 3652, 3670, 3684 and 3693 cm^{-1} . Intercalation of halloysite resulted in a Raman pattern similar to that of an

intercalated ordered kaolinite. Thus, the intercalated halloysite resembled the intercalated kaolinite at least on a molecular level [16]. Here, the conclusion was made that the intercalation process resulted in a decrease in the defect structures of the kaolinite. Based on the above examples it can be concluded that Raman spectroscopy has proven most suitable for the spectroscopic analysis of intercalated kaolinites. The difficulty in studying the thermal deintercalation of intercalates such as dimethylsulphoxide intercalated kaolinites is that of the selection of the appropriate temperatures to collect the Raman data. The objective of this research is to report the Raman spectra of the hydroxyl- and CH-stretching regions of kaolinites intercalated with dimethylsulphoxide as a function of temperature using an in-situ thermal stage and to relate these spectra to the structure of kaolinite.

2. Experimental techniques

2.1. Intercalation of kaolinites

The kaolinites used in this study were from Kiralyhegy and Szeg in Hungary. The first kaolinite is an example of an ordered or low defect kaolinite and the second of a disordered or high defect kaolinite [15,18,19]. The kaolinites were size fractionated to $<2 \mu\text{m}$. These kaolinites were intercalated by mixing 300 mg of the kaolinite in 5 cm^3 of anhydrous dimethylsulphoxide at 25°C . The mixture was stirred using a magnetic stirrer for 80 h. Raman spectra shows the presence of some water in the so-called pure ‘anhydrous’ dimethylsulphoxide. It should be noted that in the preparation of the DMSO-kaolinite intercalate by previous workers water–DMSO mixtures were used. In fact Olejnik found the optimum rate of intercalation occurred when the kaolinite was suspended in DMSO containing 9% water [20,21]

2.2. Thermoanalytical investigations

TG-MS investigation of the intercalate was carried out by means of a Netzsch TG 209 thermobalance coupled with a Balzers MSC 200 Thermo-cube type mass spectrometer connected via a fused silica capillary for sample introduction. Samples of 3 mg were

heated in a helium atmosphere at the rate of 10°C/min from ambient to 600°C. Simultaneous TG-DTG-DTA experiments were carried out in a nitrogen atmosphere in a Derivatograph PC-type (Hungarian Optical Works, Budapest) equipment connected with a selective water monitor.

2.3. Raman spectroscopy

Very small amounts of the kaolinite or the DMSO-intercalated clay mineral were placed on a polished metal surface on the stage of an Olympus BHSM microscope, equipped with 10×, 20×, and 50× objectives. The microscope is part of a Renishaw 1000 Raman microscope system, which also includes a monochromator, a filter system and a charge-coupled device (CCD). Raman spectra were excited by a Spectra-Physics model 127 He/Ne laser (633 nm) and recorded at a resolution of 2 cm⁻¹ and were acquired in sections of ≈1000 cm⁻¹ for 633 nm excitation. Repeated acquisitions using the highest magnification were accumulated to improve the signal-to-noise ratio. Spectra were calibrated using the 520.5 cm⁻¹ line of a silicon wafer. The best method of placing the kaolinites on this metal surface was to take a very small amount on the end of the spatula and then tap the crystals on to the metal surface. Further details on the spectroscopy have been published elsewhere [16,17,19].

Spectra at elevated temperatures were obtained using a Linkam thermal stage (Scientific Instruments, Waterfield, Surrey, England). Samples were placed on a circular glass disc, which fitted over the silver plate of the thermal stage. The samples were heated at 5°/min and held at the chosen temperature while accumulation of spectra occurred. The sample was then heated to the next temperature setting and the process was repeated. Because of the increased optical path, spectra above room temperature are noisier and require longer accumulation times. Spectra were obtained using 12 s scans for 20 min using the special short 20× (UWLD) objective. A lower intensity Raman signal was obtained using this objective owing to the low numerical aperture of this long working distance objective. This, combined with the spherical aberration of the stage window, results in signals of decreased intensity.

Spectral manipulation such as baseline adjustment, smoothing and normalisation was performed using the Spectralcalc software package GRAMS (Galactic Industries, NH, USA). Band component analysis was undertaken using the Jandel 'Peakfit' software package which enabled the type of fitting function to be fixed or varied accordingly. Band fitting was done using a Lorentz–Gauss cross-product function with the minimum number of component bands used for the fitting process. The Gauss–Lorentz ratio was maintained at values >0.7 and fitting was undertaken until reproducible results were obtained with squared correlations of $r^2 > 0.995$.

3. Results and discussion

3.1. Thermal analysis

Thermal analysis can reveal information about the behaviour of intercalated kaolinites. Fig. 1 shows the DTA/TGA pattern for the thermal decomposition of the low defect dimethylsulphoxide intercalated kaolinite over the temperature range 25–300°C. The figure shows the derivative thermogravimetric curve (DTG), the loss of water (H₂O), the differential ther-

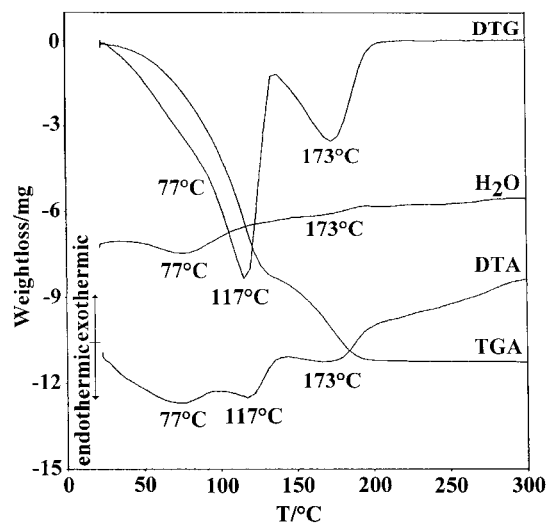


Fig. 1. Thermal analysis of DMSO intercalated low defect kaolinite.

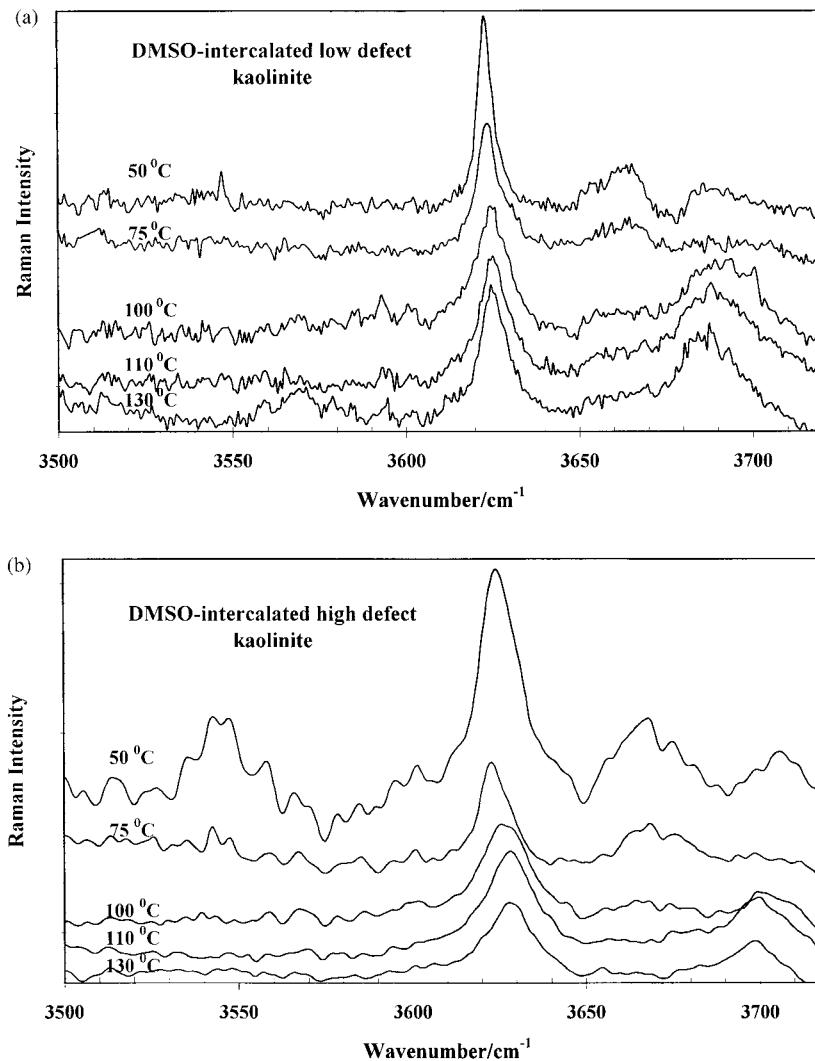


Fig. 2. Raman spectra in the hydroxyl-stretching region of the deintercalation of low defect kaolinite intercalated with DMSO. (b) Raman spectra in the hydroxyl-stretching region of the deintercalation of high defect kaolinite intercalated with DMSO.

mal analysis (DTA) curve and the thermogravimetric curve (TGA). Water is lost at two steps at 77°C and in a minor amount at 173°C. The amount of water in the intercalate is $\approx 7\%$. The DTA curve shows three endotherms at 77°, 117°, 173°C. Both the TGA and DTG curves show weight losses at 77°, 117° and 173°C. On heating the dimethylsulphoxide intercalated low defect kaolinite, two stages of loss of DMSO are observed by mass spectrometry at 117° and 173°C.

DMSO is released from the sample in two different stages representing a temperature difference of 56°C. This implies the DMSO is present in the intercalate in two completely different forms.

From the study of the thermal analysis patterns of the DMSO intercalated kaolinites, specific temperatures were chosen for Raman spectroscopic analysis. These temperatures are 50°, 75°, 100°, 110°, 130°C. The Raman spectra for the deintercalation of the low

Table 1

Results of the band component analysis of the Raman spectra at 25°, 50°, 75°, 100°, 115°, 130°C of the hydroxyl-stretching region of low defect kaolinite intercalated with dimethylsulphoxide

Temperature	Raman spectra	ν_{5b}	ν_{5a}	ν_{6a}	ν_3	ν_2	ν_4	ν_1
25°C	Band position (cm ⁻¹)		3620	3660				
	Bandwidth (cm ⁻¹)		3.7	13.0				
	Relative area (%)		38.2	61.2				
50°C	Band position (cm ⁻¹)		3622	3664			3687	3702
	Bandwidth (cm ⁻¹)		5.2	8.2			8.7	26.7
	Relative area (%)		45.9	26.9			9.7	17.4
75°C	Band position (cm ⁻¹)	3630	3622	3658		3666	3686	3702
	Bandwidth (cm ⁻¹)	7.5	6.7	18.3		10.0	12.6	16.7
	Relative area (%)	9.9	42.8	17.6		12.5	8.3	8.8
100°C	Band position (cm ⁻¹)	3628	3622	3658		3667	3686	3698
	Bandwidth (cm ⁻¹)	5.8	10.8	7.5		9.7	16.7	13.8
	Relative area (%)	5.5	38.8	3.5		3.8	34.0	14.4
115°C	Band position (cm ⁻¹)		3622		3655	3664	3685	3696
	Bandwidth (cm ⁻¹)		9.9		6.1	14.4	20.4	22.5
	Relative area (%)		40.0		2.8	7.7	34.2	15.3
130°C	Band position (cm ⁻¹)		3622		3654	3665	3685	3694
	Bandwidth (cm ⁻¹)		10.6		13.8	16.0	17.8	21.3
	Relative area (%)		40.8		6.1	10.2	29.7	13.0
Untreated kaolinite	Band position (cm ⁻¹)		3620		3650	3670	3684	3693
	Bandwidth (cm ⁻¹)		5.7		11.5	15.4	9.5	15.2
	Relative area (%)		20.8		14.5	15.4	30.0	17.7

Table 2

Results of the band component analysis of the Raman spectra at 25°, 50°, 75°, 100°, 115°, 130°C of the hydroxyl-stretching region of high defect kaolinite intercalated with dimethylsulphoxide

Temperature	Raman spectra	ν_5	ν_{6a}	ν_3	ν_2	ν_4	ν_1
25°C	Band position (cm ⁻¹)	3620	3664				3700
	Bandwidth (cm ⁻¹)	8.1	17.0				12.2
	Relative area (%)	54.0	37.0				9.0
50°C	Band position (cm ⁻¹)	3622	3666		3677		3700
	Bandwidth (cm ⁻¹)	10.6	13.2		11.6		15.6
	Relative area (%)	53.5	24.4		12.7		9.4
75°C	Band position (cm ⁻¹)	3622	3665		3675		3705
	Bandwidth (cm ⁻¹)	13.9	11.5		6.6		7.7
	Relative area (%)	71.0	18.2		4.4		5.9
100°C	Band position (cm ⁻¹)	3622	3665		3676		3702
	Bandwidth (cm ⁻¹)	16.8	9.5		12.5		14.5
	Relative area (%)	67.5	6.9		6.5		19.9
110°C	Band position (cm ⁻¹)	3625	3660		3678		3700
	Bandwidth (cm ⁻¹)	16.8	9.0		15.0		17.8
	Relative area (%)	65.6	1.7		7.4		25.3
130°C	Band position (cm ⁻¹)	3625	3662			3681	3698
	Bandwidth (cm ⁻¹)	17.4	15.0			12.5	17.3
	Relative area (%)	63.1	4.1			6.6	26.2
Untreated High defect kaolinite	Band position (cm ⁻¹)	3621	3634	3655	3675		3696
	Bandwidth (cm ⁻¹)	11.4	22.0	23.0	22.9		19.1
	Relative area (%)	18.9	6.4	9.6	10.7		39

defect and high defect kaolinites intercalated with DMSO are shown in Fig. 2(a) and (b). The results of the band component analysis of the spectra are reported in Table 1 for the low defect kaolinite intercalated with DMSO and in Table 2 for the high defect kaolinite. At 25°C, the Raman spectrum of the hydroxyl-

stretching region shows two bands only at 3620 and 3660 cm^{-1} (Fig. 3(a)). The first band is attributed to the inner hydroxyl of the kaolinite and the second to the inner surface hydroxyls hydrogen bonded to the DMSO. The relative intensities of these bands are 38.2 and 61.2%. No intensity is found in the bands attrib-

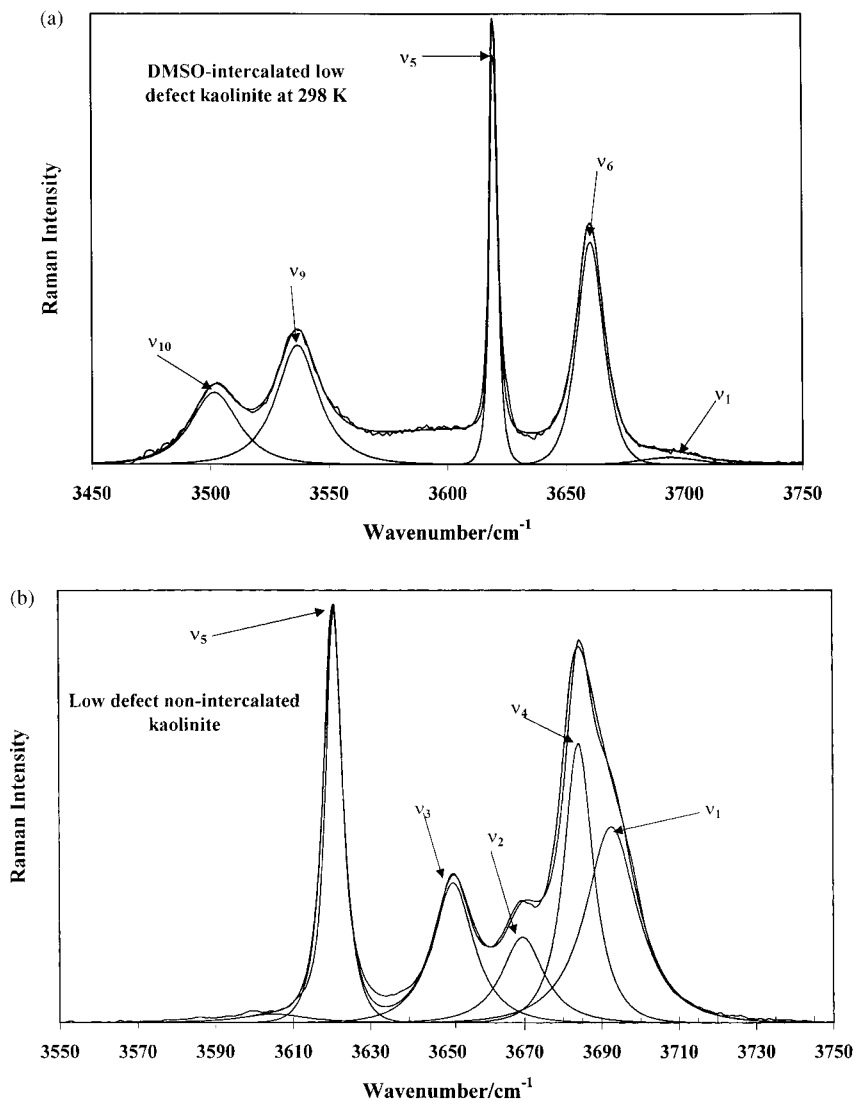


Fig. 3. (a) Band component analysis of the Raman spectrum of the hydroxyl-stretching region of low defect kaolinite intercalated with DMSO at 298 K. (b) Band component analysis of the Raman spectrum of the hydroxyl-stretching region of low defect kaolinite at 298 K. (c) Band component analysis of the Raman spectrum of the hydroxyl-stretching region of high defect kaolinite intercalated with DMSO at 298 K. (d) Band component analysis of the Raman spectrum of the hydroxyl-stretching region of high defect kaolinite at 298 K.

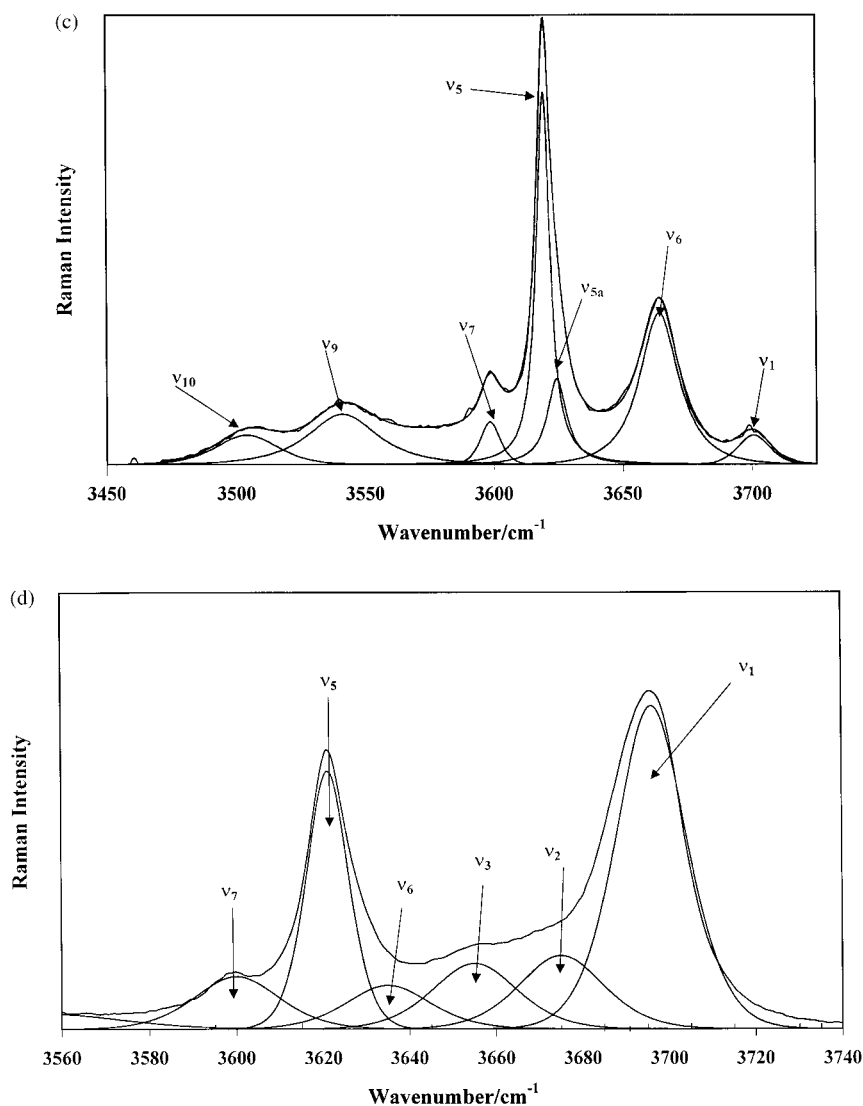


Fig. 3. (Continued)

uted to the inner surface hydroxyls of the untreated kaolinite (Fig. 3(b)). These bands are found at 3650, 3668, 3684 and 3695 cm⁻¹.

Fig. 2(a) and (b) clearly show the deintercalation of the DMSO intercalated low defect kaolinite as the temperature is increased. The fully intercalated DMSO intercalated kaolinite shows no intensity in the ν₁ to ν₄ bands. At 50°C, decomposition has commenced as is evidenced by increase in the intensity of the ν₄ band at 3687 cm⁻¹ in Fig. 2(a) and the

increase in intensity of the ν₅ band at 3702 cm⁻¹ in Fig. 2(b). As the sample is heated through the deintercalation temperatures, the intensity of the band at 3660 cm⁻¹ decreases and the intensity of the ν₁ to ν₄ bands increase in intensity. This is shown in Fig. 4(a). There is a steady decrease in intensity of the 3660 cm⁻¹ band and at the same time the ν₁ and ν₄ bands increase in intensity. The ν₅ band increases then decreases in intensity. The figure shows some change in slope ca. 110°C. This is attributed to the tempera-

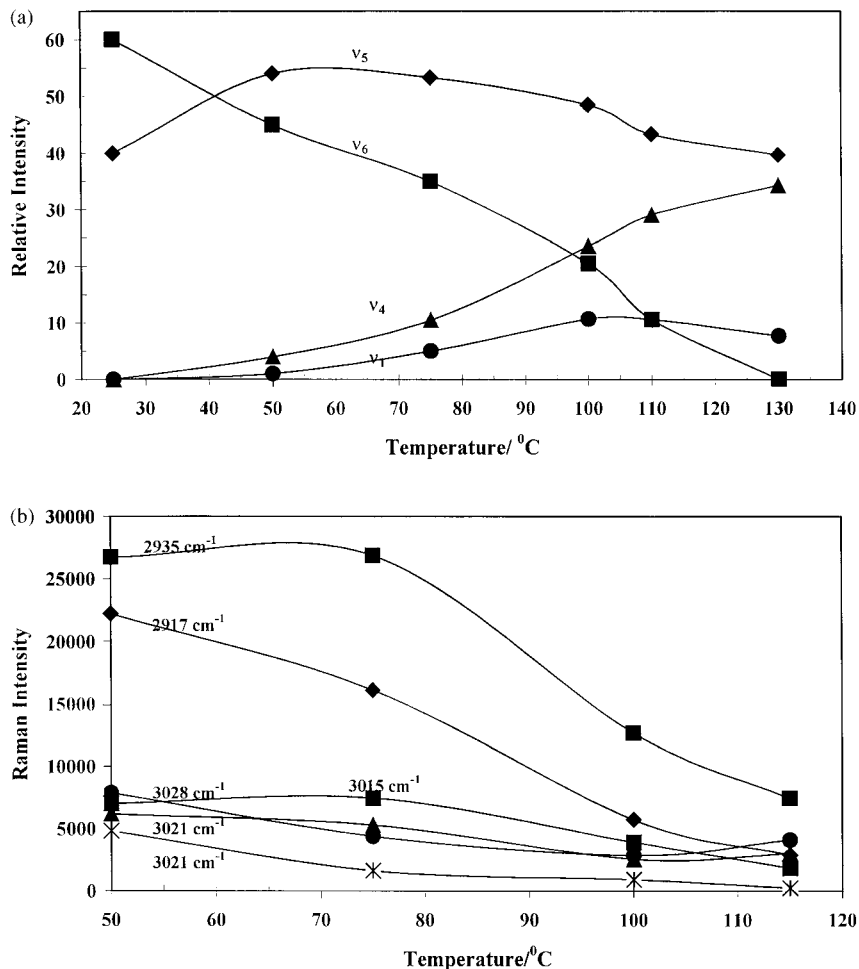


Fig. 4. Variation in the relative intensity of the hydroxyl-stretching bands of DMSO intercalated low defect kaolinite as a function of temperature. (b) Variation in the relative intensity of the CH-stretching bands of DMSO intercalated low defect kaolinite as a function of temperature.

ture at which the kaolinite starts to deintercalate. Both the Raman and DRIFT spectra of the kaolinite at 173 °C show the kaolinite to be completely deintercalated. The spectrum of the deintercalated kaolinite closely resembles that of the non-intercalated kaolinite. At 130 °C, the spectrum approaches that of the untreated kaolinite (Fig. 3(b)). The untreated kaolinite shows bands at 3693 and 3684 cm^{-1} with 17.7 and 30.0% of the relative intensity and for the thermally deintercalated kaolinite at 130 °C, the intensity of these two bands is 13.0 and 29.7%, respectively. It is interesting to observe the reformation of the Raman

bands attributed to the inner surface hydroxyls. The bands are 3702 cm^{-1} at 50 °C and are at 3693 cm^{-1} at 130 °C. Importantly the temperatures at which Raman spectra were collected were ascertained from the endotherms of the DTA patterns.

A similar set of observations is made for deintercalation by thermal treatment of the DMSO-intercalated high defect kaolinite (Fig. 3(c)). High defect kaolinites are characterised by the lack of intensity in the ν_4 band at 3684 cm^{-1} (Fig. 3(d)). Thus, no band is observed in this position in Fig. 3(c). The intensity of the inner surface hydroxyls for the ν_1 band at

Table 3

Results of the band component analysis of the Raman spectra of the CH-stretching region of low defect kaolinite intercalated with dimethylsulphoxide

Temperature	Raman spectra	ν_6	ν_5	ν_4	ν_3	ν_2	ν_1
25°C	Band position (cm ⁻¹)	2917	2935	2998	3015	3021	3029
	Bandwidth (cm ⁻¹)	76.0	7.2	6.7	6.9	7.0	7.5
	Relative area (%)	27.4	35.0	9.0	9.5	7.2	11.9
50°C	Band position (cm ⁻¹)	2917	2935	2998		3020	3029
	Bandwidth (cm ⁻¹)	8.2	6.0	10.2		19.8	4.3
	Relative area (%)	40.1	20.6	11.6		26.5	1.2
50°C	Band position (cm ⁻¹)	2917	2935	2999		3020	3029
	Bandwidth (cm ⁻¹)	6.0	6.9	5.2		15.7	4.2
	Relative area (%)	29.5	34.4	4.5		29.8	1.8
75°C	Band position (cm ⁻¹)	2918	2934	2999		3019	3029
	Bandwidth (cm ⁻¹)	7.0	8.0	6.6		11.7	7.8
	Relative area (%)	35.5	30.8	8.5		21.2	4.0
100°C	Band position (cm ⁻¹)	2918	2935	2999		3020	3028
	Bandwidth (cm ⁻¹)	7.5	9.4	5.0		13.2	5.5
	Relative area (%)	35.0	34.9	3.6		22.6	3.9
110°C	Band position (cm ⁻¹)						
	Bandwidth (cm ⁻¹)						
	Relative area (%)						
130°C	Band position (cm ⁻¹)						
	Bandwidth (cm ⁻¹)						
	Relative area (%)						
DMSO	Band position (cm ⁻¹)	2911		2996			
	Bandwidth (cm ⁻¹)	10.4		18.6			
	Relative area (%)	60.0		39.9			

Table 4

Results of the band component analysis of the Raman spectra of the CH-stretching region of high defect kaolinite intercalated with dimethylsulphoxide

Temperature	Raman spectra	ν_6	ν_{6a}	ν_5	ν_4	ν_3	ν_2	ν_1
25°C	Band position (cm ⁻¹)	2917		2935	2998	3015	3021	3029
	Bandwidth (cm ⁻¹)	76.0		7.2	6.7	6.9	7.0	7.5
	Relative area (%)	27.4		35.0	9.0	9.5	7.2	11.9
50°C	Band position (cm ⁻¹)	2920		2937	3002	3012	3021	3031
	Bandwidth (cm ⁻¹)	9.9		10.2	10.4	10.4	10.7	11.4
	Relative area (%)	31.6		25.5	9.5	2.9	10.0	9.0
75°C	Band position (cm ⁻¹)	2920		2937	3002	3012	3021	3031
	Bandwidth (cm ⁻¹)	10.2		11.0	9.6	10.0	11.5	11.8
	Relative area (%)	34.2		31.6	7.4	2.4	11.2	8.0
100°C	Band position (cm ⁻¹)	2921	2928	2937	3002	3012	3021	3031
	Bandwidth (cm ⁻¹)	10.5	8.0	11.5	10.0	9.0	11.1	12.2
	Relative area (%)	34.8	1.0	32.3	7.5	2.5	10.6	9.3
110°C	Band position (cm ⁻¹)	2920	2928	2936	3002	3012	3020	3031
	Bandwidth (cm ⁻¹)	10.8	8.0	11.6	10.5	9.8	11.4	12.3
	Relative area (%)	29.9	4.9	24.5	6.4	4.0	6.3	11.1
130°C	Band position (cm ⁻¹)	2920	2927	2937	3002	3012	3021	3031
	Bandwidth (cm ⁻¹)	10.5	7.9	11.5	10.2	9.5	12.9	13.2
	Relative area (%)	32.3	10.6	18.0	5.5	3.2	2.0	4.0
DMSO	Band position (cm ⁻¹)	2911			2996			
	Bandwidth (cm ⁻¹)	10.4			18.6			
	Relative area (%)	60.1			39.9			

3695 cm^{-1} for the untreated high defect kaolinite makes up 39% of the total intensity. The ν_{6a} 3664 cm^{-1} band makes up 37% of the total band intensity at 25°C . This value corresponds well with that for the untreated kaolinite. This suggests that the two bands are the same. This band intensity for the dimethylsulphoxide intercalated high defect kaolinite decreases to 24.4% at 50°C , 18.2% at 75°C and 6.9% at 100°C . This decrease in intensity is attributed to the inner surface hydroxyls hydrogen bonded to the DMSO and the band is observed at slightly higher

position than that (3660 cm^{-1}) of the DMSO intercalated low defect kaolinite. This small difference is attributed to the strength of the hydrogen bond formed between the inner surface hydroxyls and the DMSO molecule. The inner hydroxyl band at 3620 cm^{-1} shows a blue shift towards 3625 cm^{-1} upon thermal treatment. This shift is considered to be related to the folding of the kaolinite layers of the high defect kaolinite. Another observation is that the spectrum at 130°C shows some intensity in the ν_4 band. The significance of this rests with the reordering of the

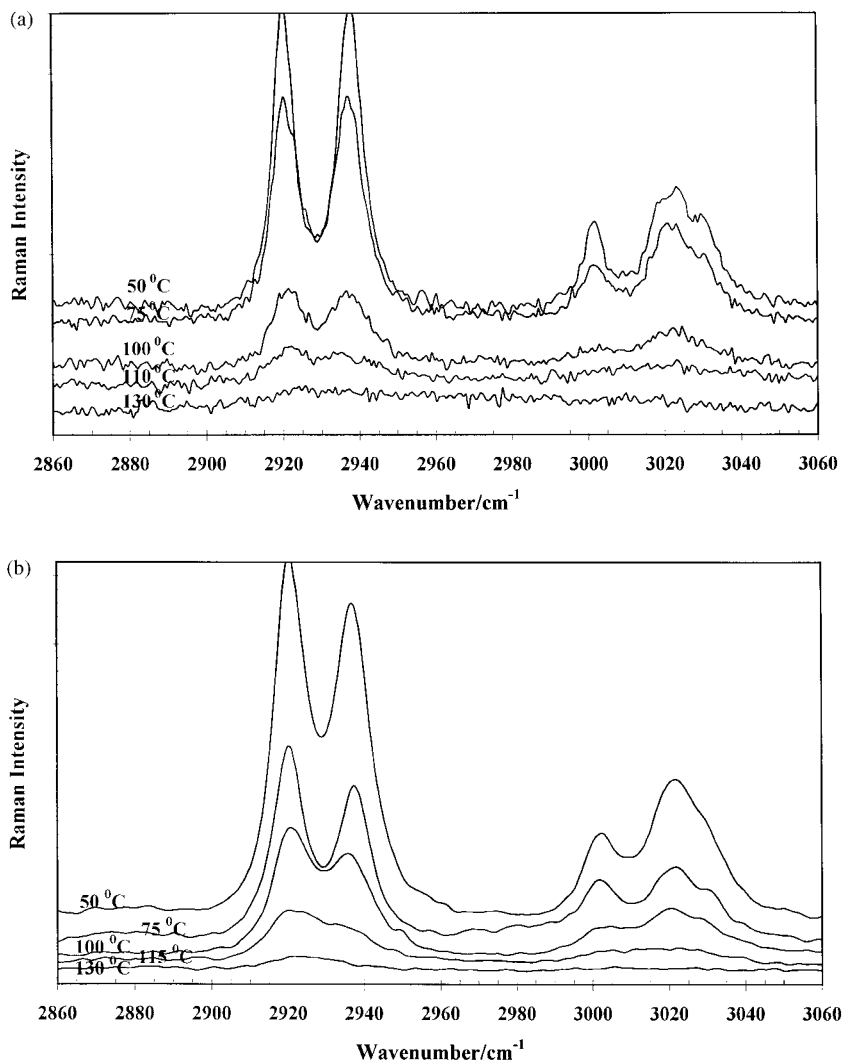


Fig. 5. Raman spectra in the CH-stretching region of the deintercalation of low defect kaolinite intercalated with DMSO. (b) Raman spectra in the CH-stretching region of the deintercalation of high defect kaolinite intercalated with DMSO.

kaolinite layers. Upon intercalation of the high defect kaolinite with DMSO followed by deintercalation, the defect structures in the kaolinite (stacking disorder) have decreased and the spectrum is similar to that of the low defect kaolinite.

The deintercalation of the DMSO intercalated kaolinites may also be followed by the decrease in intensity of the CH-stretching modes in the 2900–3050 cm^{-1} region. Fig. 4(a) and (b) illustrate this deintercalation. Tables 3 and 4 report the band component analysis of the CH-stretching region of the DMSO-intercalated low and high defect kaolinites, respectively. The DMSO shows two simple Raman bands at 2911 and 2996 cm^{-1} . These bands are attributed to the symmetric and antisymmetric stretching vibrations of the CH of the methyl group. Fig. 5(a) and (b) show that upon intercalation, the 2911 cm^{-1} band splits into two bands at 2917 and 2935 cm^{-1} . This splitting is attributed to a loss of degeneracy. The 2917 cm^{-1} band is the less intense of the two bands in the Raman spectra, being the symmetric stretching mode. The two bands show that there are two different methyl groups in the DMSO intercalated kaolinite one of which is perturbed to high frequency. Such a loss of degeneracy was proposed by Johnston but the spectra of Johnston show a lack of intensity in the 2935 cm^{-1} band, which may be attributed to the partial intercalation of the kaolinite [21]. The 2996 cm^{-1} band loses its degeneracy upon intercalation and thus four bands are observed at 2998, 3015, 3021, and 3029 cm^{-1} . Significant intensity remains in these bands even at 110°C. Only at 130°C is there no intensity remaining. This means that some of the DMSO is retained in the intercalated complex at 110°C and at 130°C all of the DMSO has been lost.

4. Conclusion

The TG-MS investigation of the intercalate enabled the thermal characteristics of the deintercalation of the DMSO intercalated kaolinite to be obtained. Three endotherms were observed at 77°, 117° and 173°C which were attributed to the loss of water and the loss of DMSO in two stages. It is proposed that the DMSO in the intercalate exists in two different forms. The thermal analysis data was used to select appropriate temperatures for the collection of Raman spectral data.

The significance of this paper rests with the use of the thermal stage for the study of deintercalation of DMSO intercalated kaolinites and the determination of selected temperatures from the DTA patterns for Raman spectral analysis. The use of a thermal stage enabled Raman spectra of the deintercalation process to be obtained in situ at elevated temperatures. The technique of using the thermal stage has wide application to many physical processes such as adsorption/desorption, catalytic activity, dehydration, dehydroxylation and phase changes. In this example, deintercalation can be followed by the decrease in intensity of the bands attributed to the hydroxyl stretching and CH stretching. The Raman spectra of the DMSO intercalated kaolinites show two bands at 3620 and 3660 cm^{-1} for the DMSO intercalated low defect kaolinite and 3620 and 3664 cm^{-1} for the high defect intercalated kaolinite. The 3620 cm^{-1} band is attributed to the inner hydroxyl of the kaolinite and shows no change upon deintercalation. Importantly the 3660 and 3664 cm^{-1} bands are attributed to the inner surface hydroxyls of the kaolinite hydrogen bonded to the DMSO. Significantly, after deintercalation, the structure of the kaolinite returned to its original structure, at least on the molecular scale.

Acknowledgements

The financial and infra-structural support of the Queensland University of Technology, Centre for Instrumental and Developmental Chemistry is gratefully acknowledged. One of the authors (RLF) is grateful for the invitation to undertake study leave at the Luleå University of Technology. Financial support from the Hungarian Scientific Research Fund under grant OTKA T25171 is also acknowledged.

References

- [1] G. Lagaly, *Phil Trans. R. Soc. Lond.* A311 (1984) 315.
- [2] A. Weiss, W. Thielepape, H. Orth, Intercalation into kaolinite minerals, in: L. Heller, A. Weiss (Eds.), *Proc. Int. Clay Conf. Jerusalem I*, Jerusalem: Israel University Press, 1966, p. 277.
- [3] G.J. Churchman, *Clays Clay Miner.* 38 (1990) 591.
- [4] L. Heller-Kallai, E. Huard, R. Prost, *Clay Miner.* 26 (1991) 245.

- [5] I. Lapidés, N. Lahav, K.H. Michaelian, S. Yariv, *J. Therm. Anal.* 49 (1997) 1423.
- [6] N. Lahav, *Clays Clay Miner.* 38 (1990) 219.
- [7] M. Raupach, P.F. Barron, J.G. Thompson, *Clays Clay Miner.* 35 (1987) 208.
- [8] J.G. Thompson, C. Cuff, *Clays Clay Miner.* 33 (1985) 490.
- [9] J.G. Thompson, *Clays Clay Miner.* 33 (1985) 173.
- [10] S. Hayashi, *Clays Clay Miner.* 45 (1997) 724.
- [11] S. Hayashi, *J. Phys. Chem.* 99 (1995) 7120.
- [12] P.M. Costanzo, R.F. Giese, C.V. Clemency, *Clays Clay Miner.* 32 (1984) 29.
- [13] P.M. Costanzo, R.F. Giese, *Clays Clay Miner.* 34 (1986) 105.
- [14] P.M. Costanzo, R.F. Giese, *Clays Clay Miner.* 38 (1990) 160.
- [15] J. Kristof, R.L. Frost, A. Felinger, J. Mink, *J. Molec. Struct.* 41 (1997) 119.
- [16] R.L. Frost, T.H. Tran, J. Kristof, *Clay Miner.* 32 (1997) 587.
- [17] R.L. Frost, J. Kristof, *Clays Clay Miner.* 45 (1997) 68.
- [18] J. Kristof, M. Toth, M. Gabor, P. Szabo, R.L. Frost, *J. Therm. Anal.* 49 (1997) 1441.
- [19] R.L. Frost, T.H. Tran, L. Rintoul, J. Kristof, *The Analyst* 123 (1998) 611.
- [20] S. Olejnik, L.A.G. Aylmore, A.M. Posner, J.P. Quirk, *J. Phys. Chem.* 72 (1968) 241.
- [21] C.T. Johnston, G. Sposito, D.F. Bocian, R.R. Birge, *J. Phys. Chem.* 88 (1984) 5959.